64. Lowry T. H. and Richardson, K. S., *Mechanism and Theory in Organic Chemistry*, (Harper and Row, New York, 1976).
65. Baer T. and Carney, T. E., *J. Chem. Phys.* **76**, 1304 (1982).
66. Proch, D., Rider, D. M., and Zare, R. N., *Chem. Phys. Lett.* **81**, 430 (1981); Kühlewind, H., Neusser, H. J., and Schlag, E. W., *J. Chem. Phys.* **82**, 5452 (1985).
67. Clark, T., *J. Am. Chem. Soc.* **110**, 1672 (1988); Illies, A. J., Livant, P., and McKee, M. L., *J. Am. Chem. Soc.* **110**, 7980 (1988).
68. Asmus, K.-D., *Acct. Chem. Res.* **12**, 436 (1979).
69. Naito, A., Akasaka, K., and Hatano, H., *Mol. Phys.* **44**, 427 (1981).
70. Block, E., *Reactions of Organosulfur Compounds*, (Academic Press, New York, 1978), Chap. 4.
71. Drewello, T., Lebrilla, C. B., Schwarz, H., de Koning, L. J., Fokkens, R. H., Nibbering, N. M. M., Anklam, E., and Asmus, K.-D., *J. Chem. Soc. Chem. Commun.*, 1381 (1987); Musker, W. K., Gorewit, B. V., Roush, P. B., and Wolford, T. L., *J. Org. Chem.* **43**, 3235 (1978).
72. Syage, J. A., Pollard, J. E., and Cohen, R. B., *Appl. Opt.* **26**, 3516 (1987).
73. Csizmadia, I. G., Duke, A. J., Lucchini, V., and Modena, G., *J. Chem. Soc. Perkin Trans. II*, 1808 (1974).
74. Capozzi, G., DeLucchi, O., Lucchini, V., and Modena, G., *Chem. Commun.*, 248 (1975).
75. Möckel, H. J., *Fresenius Z. Anal. Chem.* **295**, 241 (1979).

12. Quantum Brownian Oscillator Analysis of Pump-Probe Spectroscopy in the Condensed Phase

YOSHITAKA TANIMURA and SHAUL MUKAMEL
Department of Chemistry, University of Rochester, Rochester, New York 14627, U.S.A.

1. Introduction

Nuclear motions and relaxation play an important role in determining the rates and outcomes of chemical processes in the condensed phase [1–12]. Electron transfer, isomerization and bimolecular reactions are directly effected by intramolecular vibrations as well as solvent motions.

Femtosecond spectroscopy allows the direct probe of elementary nuclear motions [11, 13]. Much physical insight can be gained by formulating nonlinear spectroscopy in terms of nonlinear response functions which are given as sums of contributions of Liouville space paths [14]. Each of these paths may be represented using a nuclear wavepacket in phase space. Comparison of the wavepackets with the experimental observable allows the development of a powerful semiclassical representation of nonlinear spectroscopy. The nonlinear response functions obtained from nonlinear spectroscopies can then be used to calculate other processes including curve crossing and electron transfer [15, 16, 17].

The multimode Brownian oscillator model provides a convenient means for incorporating nuclear degrees of freedom in the response function [14]. We have recently used a path integral approach [18] to develop exact closed expressions for the nuclear wavepackets in phase space and nonlinear response functions for this model [19] (hereafter denoted TM). In this paper, we apply these results to the analysis of pump-probe spectroscopy. In Section 2, we introduce the response functions and present expressions for the wavepackets using the Condon approximation which neglects the variation of the transition dipole moment with nuclear coordinates. More general expressions which do not involve the Condon approximation are given in the Appendix. In Section 3, we apply these results to impulsive pump-probe spectroscopy and analyze the roles of high frequency (underdamped) modes as well as overdamped solvation modes.

J.D. Simon (ed.), Ultrafast Dynamics of Chemical Systems, 327–343.

2. Phase Space Wavepacket Representation for the Optical Response

We consider a two electronic level system with a ground state $|g>$ and an excited state $|e>$ interacting with an external electromagnetic field $E(t)$;

$$H_s = H_0 - E(t)V, \tag{2.1}$$

where

$$H_0 = |g> H_g < g| + |e> H_e < e|, \tag{2.2}$$

with

$$\begin{cases} H_g = \frac{p^2}{2M} + U_g(q), \\ H_e = \frac{p^2}{2M} + U_e(q), \end{cases} \tag{2.3}$$

and p, q, and M represent the momentum, the coordinate and the mass of a nuclear coordinate, respectively. V is the dipole operator which is given by

$$V = |g> \mu(q) < e| + |e> \mu(q) < g|. \tag{2.4}$$

$\mu(q)$ is the dipole matrix element between the two states which depends on the nuclear coordinate. The potentials of the excited and the ground states are assumed to be harmonic:

$$\begin{cases} U_g(q) = \frac{1}{2}M\omega_0^2 q^2, \\ U_e(q) = \frac{1}{2}M\omega_0^2(q+D)^2 + \hbar\omega_{eg}^0, \end{cases} \tag{2.5}$$

where ω_{eg}^0 is the electronic energy gap and D is the displacement of the potential. This system is embedded in a solvent, which is modelled as a set of harmonic oscillators with coordinates x_n and momenta p_n. The interaction between the system and the n-th oscillator is assumed to be linear with a coupling strength c_n. The total Hamiltonian is then given by [20, 21]

$$H = H_s + H', \tag{2.6}$$

where

$$H' = \sum_n \left[\frac{p_n^2}{2m_n} + \frac{m_n\omega_n^2}{2}\left(x_n - \frac{c_n q}{m_n\omega_n^2}\right)^2 \right]. \tag{2.7}$$

We assume the entire system is initially at equilibrium in the ground electronic state:

$$\rho_g = |g><g| \exp[-\beta(H_g + H')]/\mathrm{Tr}\{\exp[-\beta(H_g + H')]\}, \tag{2.8}$$

where $\beta \equiv 1/k_B T$ is the inverse temperature. All effects of the heat bath on the system are determined by a spectral distribution of coupling strength defined by

$$J(\omega) = \pi \sum_n \frac{c_n^2}{2m_n\omega_n}\delta(\omega - \omega_n). \tag{2.9}$$

By introducing a frequency dependent friction, $\tilde{\gamma}(\omega) \equiv J(\omega)/\omega$, the anti-symmetric and a symmetric equilibrium correlation functions of the nuclear coordinate are expressed as

$$\begin{aligned} \chi(t) &\equiv \frac{i}{\hbar}\langle q(t)q - qq(t)\rangle_g \\ &= \frac{1}{M}\int_{-\infty}^{\infty}\frac{d\omega}{\pi}\frac{\omega\tilde{\gamma}(\omega)}{(\omega_0^2 - \omega^2)^2 + \omega^2\tilde{\gamma}^2(\omega)}\sin(\omega t), \end{aligned} \tag{2.10}$$

and

$$\begin{aligned} S(t) &\equiv \frac{1}{2}\langle q(t)q + qq(t)\rangle_g \\ &= \frac{\hbar}{M}\int_{-\infty}^{\infty}\frac{d\omega}{2\pi}\frac{\omega\tilde{\gamma}(\omega)}{(\omega_0^2 - \omega^2)^2 + \omega^2\tilde{\gamma}^2(\omega)}\coth\left(\frac{\beta\hbar\omega}{2}\right)\cos(\omega t). \end{aligned} \tag{2.11}$$

We further introduce the auxiliary function

$$g_\pm(t) \equiv \xi^2\int_0^t dt'\int_0^{t'} dt''\left[S(t'') \pm \frac{i\hbar}{2}\chi(t'')\right], \tag{2.12}$$

where

$$\xi \equiv \frac{MD\omega_0^2}{\hbar} = d\sqrt{\frac{M\omega_0^3}{\hbar}} = \frac{2\lambda}{d}\sqrt{\frac{\hbar}{M\omega_0}}. \tag{2.13}$$

Here, we defined the dimensionless nuclear displacement parameter, $d \equiv D\sqrt{M\omega_0/\hbar}$, and the Stokes shift parameter

$$\lambda \equiv \frac{MD^2\omega_0^2}{2\hbar} = \frac{d^2\omega_0}{2}. \tag{2.14}$$

The optical response can be expressed in terms of the optical polarization

$$P(t) \equiv \mathrm{Tr}\left\{(|e><g| + |g><e|)\int dp\int dq\mu(q)W(p,q,t)\right\}, \tag{2.15}$$

where $W(p,q,t)$ is a phase space wavepacket which depends on the interaction between the driving field and the system. Denoting the nuclear wavepacket to n-th order in the field by $W^{(n)}(p,q,t)$, we have

$$P^{(n)}(t) = \int dp \int dq \mu(q) W^{(n)}(p,q,t), \tag{2.16}$$

and

$$W(p,q,t) = \sum_n \sum_\alpha W_\alpha^{(n)}(p,q,t), \tag{2.17}$$

where $W_\alpha^{(n)}$ is the contribution of the α-th path to the n-th order polarization.

Since the equations are simpler in the Condon approximation, $\mu(q) = \mu$, we first give the expressions for this case. From TM, the first order distribution function is given by

$$W_1^{(1)}(p,q,t) = \int_0^\infty dt_1 E(t-t_1)\mu^2(4\pi^2\langle p^2\rangle_g\langle q^2\rangle_g)^{-1/2} \times \exp\left[-\frac{1}{2\langle q^2\rangle_g}(q-\bar{q}_1^{(1)}(t_1))^2 - \frac{1}{2\langle p^2\rangle_g}(p-\bar{p}_1^{(1)}(t_1))^2\right] \times R_1^{(1)}(t_1) + c.c., \tag{2.18}$$

where

$$\langle q^2\rangle_g = \xi^2\ddot{g}_+(0), \quad \langle p^2\rangle_g = \xi^{-2}M^2 d^4 g_+(t)/dt^4\,|_{t=0}, \quad \omega_{eg} \equiv \omega_{eg}^0 + \lambda, \tag{2.19}$$

and the center of the coordinate and the momentum of distribution function are given by

$$\bar{q}_1^{(1)}(t_1) = -i\xi^{-1}\dot{g}_-(t_1), \quad \bar{p}_1^{(1)}(t_1) = -iM\xi^{-1}\ddot{g}_-(t_1). \tag{2.20}$$

The first order response functions is given by

$$R_1^{(1)}(t_1)\exp[Q_1^{(2)}(t_1)], \tag{2.21}$$

where

$$Q_1^{(2)}(t_1) = -i\omega_{eg}t_1 - g_-(t_1). \tag{2.22}$$

The linear polarization is then expressed by using the response function, Equation (2.21), as

$$P^{(1)}(t) = -i\mu^2 \int_0^\infty dt_1 E(t-t_1)R_1^{(1)}(t_1) + c.c. \tag{2.23}$$

For the third order polarization, we need distribution functions for four Liouville space paths [11], $eg \to ee \to eg$, $ge \to ee \to eg$, $ge \to gg \to eg$ and $eg \to gg \to eg$ denoted by α =1–4, respectively. The corresponding phase space wavepackets are then given by

$$W^{(3)}(p,q,t) = \int_0^\infty dt_1 \int_0^\infty dt_2 \int_0^\infty dt_3 E(t-t_3)E(t-t_2-t_3) E(t-t_1-t_2-t_3)\mu^3(4\pi^2\langle p^2\rangle_g\langle q^2\rangle_g)^{-1/2} \times \sum_{\alpha=1}^4 \exp\left[-\frac{1}{2\langle q^2\rangle_g}(q-\bar{q}_\alpha^{(3)}(t_3,t_2,t_1))^2 - \frac{1}{2\langle p^2\rangle_g}(p-\bar{p}_\alpha^{(3)}(t_3,t_2,t_1))^2\right] \times R_\alpha^{(3)}(t_3,t_2,t_1) + c.c., \tag{2.24}$$

where

$$\begin{cases} \bar{q}_1^{(3)}(t_3,t_2,t_1) = -i\xi^{-1}[\dot{g}_-(t_1+t_2+t_3) - \dot{g}_+(t_2+t_3) - \dot{g}_+(t_3)], \\ \bar{q}_2^{(3)}(t_3,t_2,t_1) = -i\xi^{-1}[-\dot{g}_+(t_1+t_2+t_3) + \dot{g}_-(t_2+t_3) + \dot{g}_+(t_3)], \\ \bar{q}_3^{(3)}(t_3,t_2,t_1) = -i\xi^{-1}[-\dot{g}_+(t_1+t_2+t_3) + \dot{g}_+(t_2+t_3) + \dot{g}_-(t_3)], \\ \bar{q}_4^{(3)}(t_3,t_2,t_1) = -i\xi^{-1}[\dot{g}_-(t_1+t_2+t_3) - \dot{g}_-(t_2+t_3) + \dot{g}_-(t_3)], \end{cases} \tag{2.25}$$

and

$$\begin{cases} \bar{p}_1^{(3)}(t_3,t_2,t_1) = -iM\xi^{-1}[\ddot{g}_-(t_1+t_2+t_3) - \ddot{g}_+(t_2+t_3) + \ddot{g}_+(t_3)], \\ \bar{p}_2^{(3)}(t_3,t_2,t_1) = -iM\xi^{-1}[-\ddot{g}_+(t_1+t_2+t_3) + \ddot{g}_-(t_2+t_3) + \ddot{g}_+(t_3)], \\ \bar{p}_3^{(3)}(t_3,t_2,t_1) = -iM\xi^{-1}[-\ddot{g}_+(t_1+t_2+t_3) + \ddot{g}_+(t_2+t_3) + \ddot{g}_-(t_3)], \\ \bar{p}_4^{(3)}(t_3,t_2,t_1) = -iM\xi^{-1}[\ddot{g}_-(t_1+t_2+t_3) - \ddot{g}_-(t_2+t_3) + \ddot{g}_-(t_3)]. \end{cases} \tag{2.26}$$

The third order response function is now given by

$$R_\alpha^{(3)}(t_3,t_2,t_1) = \exp[Q_\alpha^{(4)}(t_3,t_2,t_1)], \tag{2.27}$$

where

$$\begin{cases} Q_1^{(4)}(t_3,t_2,t_1) = -i\omega_{eg}(t_1+t_3) - g_-(t_1) - g_+(t_3) \\ \qquad -[g_+(t_2) - g_+(t_2+t_3) - g_-(t_1+t_2) + g_-(t_1+t_2+t_3)], \\ Q_2^{(4)}(t_3,t_2,t_1) = -i\omega_{eg}(-t_1+t_3) - g_+(t_1) - g_+(t_3) \\ \qquad +[g_-(t_2) - g_-(t_2+t_3) - g_+(t_1+t_2) + g_+(t_1+t_2+t_3)], \\ Q_3^{(4)}(t_3,t_2,t_1) = -i\omega_{eg}(-t_1+t_3) - g_+(t_1) - g_-(t_3) \\ \qquad +[g_+(t_2) - g_+(t_2+t_3) - g_+(t_1+t_2) + g_+(t_1+t_2+t_3)], \\ Q_4^{(4)}(t_3,t_2,t_1) = -i\omega_{eg}(t_1+t_3) - g_-(t_1) - g_-(t_3) \\ \qquad -[g_-(t_2) - g_-(t_2+t_3) - g_-(t_1+t_2) + g_-(t_1+t_2+t_3)]. \end{cases} \tag{2.28}$$

Then, using the response function Equation (2.27), we have the third-order polarization in the form;

$$P^{(3)}(t) = i\mu^4 \sum_{\alpha=1}^{4} \int_0^\infty dt_3 \int_0^\infty dt_2 \int_0^\infty dt_1 E(t-t_3)E(t-t_2-t_3) E(t-t_1-t_2-t_3)R_\alpha^{(3)}(t_3,t_2,t_1) + c.c. \quad (2.29)$$

These quantities are generalized to the non-Condon case [19] and the results are given in the Appendix.

The Brownian oscillator model provides a picture in terms of wave packets in phase space which can be calculated semiclassically. Using a classical Langevin equation, Yan and Mukamel derived closed expressions for the wavepackets [22]. The equations presented here generalize these results in two aspects. (i) We use a microscopic description of the bath which provides a consistent treatment of relaxation and dephasing at all temperatures. The Langevin equation used earlier is valid at high temperatures. Yan and Mukamel have shown how the exact expression for the response function can be obtained from the Langevin equation by further assuming the cumulant expansion and including the fluctuation dissipation theorem. However, the expression of the wavepackets was given only in the high temperature limit, since the semi-classical Langevin equation approach cannot keep track of the quantum coherence between the system and the noise source (the heat bath). This coherence is less important at high temperatures due to the fast dephasing, but becomes dominant at low temperatures. (ii) We allow for an arbitrary dependence of the transition dipole moment on nuclear coordinates and thus relax the Condon approximation.

3. Impulsive Pump-Probe Spectroscopy with Non-Condon Dipole Moment

We assume the variation of the transition dipole with the nuclear coordinate (non-Condon effects) is given in the form

$$\mu(q) = \mu_0 \exp(cq). \quad (3.1)$$

We may calculate the response functions and the phase space distribution functions for this model by replacing all c_j in the Appendix by c.

In a pump-probe experiment, the system is first subjected to a short pump pulse, then after a delay τ, a second probe pulse interacts with the system. The external electric field is given by

$$E(t) = E_1(t+\tau)\exp(-i\Omega_1 t) + E_1^*(t+\tau)\exp(i\Omega_1 t) + E_2(t)\exp(-i\Omega_2 t) + E_2^*(t)\exp(i\Omega_2) \quad (3.2)$$

where $E_1(t)$ and $E_2(t)$ are the temporal envelopes, and Ω_1 and Ω_2 are the center frequency of the pump and the probe field, respectively.

The probe absorption spectrum is [14]

$$S(\Omega_1,\Omega_2;\omega_2,\tau) = -2 \operatorname{Im} E_2[\omega_2]P^{(3)}[\omega_2], \quad (3.3)$$

where

$$E_2[\omega_2] = \frac{1}{\sqrt{2\pi}} \int_{-\infty}^{\infty} dt \exp[i(\omega_2-\Omega_2)t]E_2(t), \quad (3.4)$$

and

$$P^{(3)}[\omega_2] = \frac{1}{\sqrt{2\pi}} \int_{-\infty}^{\infty} dt \exp[i(\omega_2-\Omega_2)t]P^{(3)}(t). \quad (3.5)$$

We shall assume impulsive pump and probe pulses [23]

$$E_1(t) = \theta_1\delta(t+\tau), \quad E_2(t) = \theta_2\delta(t), \quad (3.6)$$

where θ_1 and θ_2 are the pump and pulse areas, respectively. We shall calculate separately the particle contribution corresponding to the Liouville paths $\alpha = 1$ $(eg \to ee \to eg)$ and $\alpha = 2$ $(ge \to ee \to eg)$ and the hole contribution corresponding to the Liouville path $\alpha = 3$ $(ge \to gg \to eg)$ and $\alpha = 4$ $(eg \to gg \to eg)$. For the impulsive pump case, $R_1^{(3)}(t,\tau,0) = R_2^{(3)}(t,\tau,0)$ and $R_3^{(3)}(t,\tau,0) = R_4^{(3)}(t,\tau,0)$, and we have

$$S(\omega_2-\Omega_2) = S_{ee}(\omega_2-\Omega_2;\tau) + S_{gg}(\omega_2-\Omega_2;\tau). \quad (3.7)$$

Here, S_{ee} and S_{gg} are the contributions of the particle

$$S_{ee}(\omega_2-\Omega_2) = 2\operatorname{Re}\int_0^\infty dt \exp[i(\omega_2-\Omega_2)t]R_1^{(3)}(t,\tau,0), \quad (3.8)$$

and the hole, given by

$$S_{gg}(\omega_2-\Omega_2) = 2\operatorname{Re}\int_0^\infty dt \exp[i(\omega_2-\Omega_2)t]R_3^{(3)}(t,\tau,0), \quad (3.9)$$

and we set $\mu_0\theta_1 = \mu_0\theta_2 = 1$.

We have also calculated the linear absorption spectra defined by

$$\sigma(\omega) = \int_0^\infty dt\, R_1^{(1)}(t)\exp(i\omega t) + c.c. \quad (3.10)$$

Hereafter we assume a frequency independent damping, where $\gamma(\omega) = \gamma$, analytical expressions for the symmetric and antisymmetric correlation functions are known [21]. The auxiliary function is then given by

$$g_\pm(t) = g'(t) \pm ig''(t), \quad (3.11)$$

where

$$g'(t) = \lambda\left\{\left[\frac{\lambda_1^2}{2\zeta\omega_0^2}(e^{-\lambda_2 t} + \lambda_2 t - 1)\coth\left(\frac{i\beta\hbar\lambda_2}{2}\right)\right.\right.$$
$$\left.\left. - \frac{\lambda_2^2}{2\zeta\omega_0^2}(e^{-\lambda_1 t} + \lambda_1 t - 1)\coth\left(\frac{i\beta\hbar\lambda_1}{2}\right)\right]\right.$$
$$\left. - \frac{4\gamma\omega_0^2}{\beta\hbar}\sum_{n=1}^{\infty}\frac{1}{\nu_n}\frac{e^{-\nu_n t} + \nu_n t - 1}{(\omega_0^2 + \nu_n^2)^2 - \gamma^2\nu_n^2}\right\}, \tag{3.12}$$

and

$$ig''(t) = i\lambda\left[e^{-\gamma t/2}\left(\frac{\gamma^2/2 - \omega_0^2}{\zeta\omega_0^2}\sin(\zeta t) + \frac{\gamma}{\omega_0^2}\cos(\zeta t)\right) + t - \frac{\gamma}{\omega_0^2}\right]. \tag{3.13}$$

Here, we defined $\nu_n = 2\pi n/\hbar\beta$ and

$$\lambda_1 = \frac{\gamma}{2} + i\zeta, \quad \lambda_2 = \frac{\gamma}{2} - i\zeta, \quad \zeta = \sqrt{\omega_0^2 - \gamma^2/4}. \tag{3.14}$$

In the following, we present the linear absorption spectrum $\sigma(\omega)$, the pump-probe spectrum $S(\omega)$, and the second order wavepackets $W^{(2)}(t)$. The second order wavepackets with the Condon and the non-Condon interactions are obtained from Equations (2.24) and (A11), respectively, by putting $t_3 = 0$, $t_2 = t$, *i.e.* $W^{(2)}(t_1, t) = W^{(3)}(t_1, t, 0)$. For the results of the pump-probe spectrum and the wavepackets, we separately present the contribution from the particle and the hole. Calculations are performed for the Condon case ($c = 0$) and the non-Condon case ($c = 0.1$), and are denoted by a) and b) in all figures. The frequency and the dimensionless displacement are taken to be $\omega_0 = 600$ [cm^{-1}], $d = 1.0$, and $T = 100$ [K].

Figure 1 shows the linear absorption spectra calculated using Equation (3.10) for different choices of γ: 1) the underdamped case, $\gamma = 40$ [cm^{-1}]; 2) the intermediate case $\gamma = 400$ [cm^{-1}]; and 3) the overdamped case $\gamma = 2000$ [cm^{-1}]. The non-Condon spectra are slightly shifted to the blue compared with the Condon spectra. This shift becomes larger as the temperature is increased. The reason is as follows; prior to the pump excitation, the system is in the ground equilibrium state and the nuclear wavepacket, which is well localized if the temperature is low, broadens at high temperatures. As seen from Equation (3.1) the dipole element $\mu(q)$ is a linear function of q for small c. The probability of the system to have large nuclear displacements q increases with temperature, and the non-Condon effect becomes therefore larger at higher temperatures. Since $\mu(q)$ becomes larger where the excitation energy between the ground state and the excitation state is high, then it helps the excitation of the pump and, thus, the spectrum shifts to the blue.

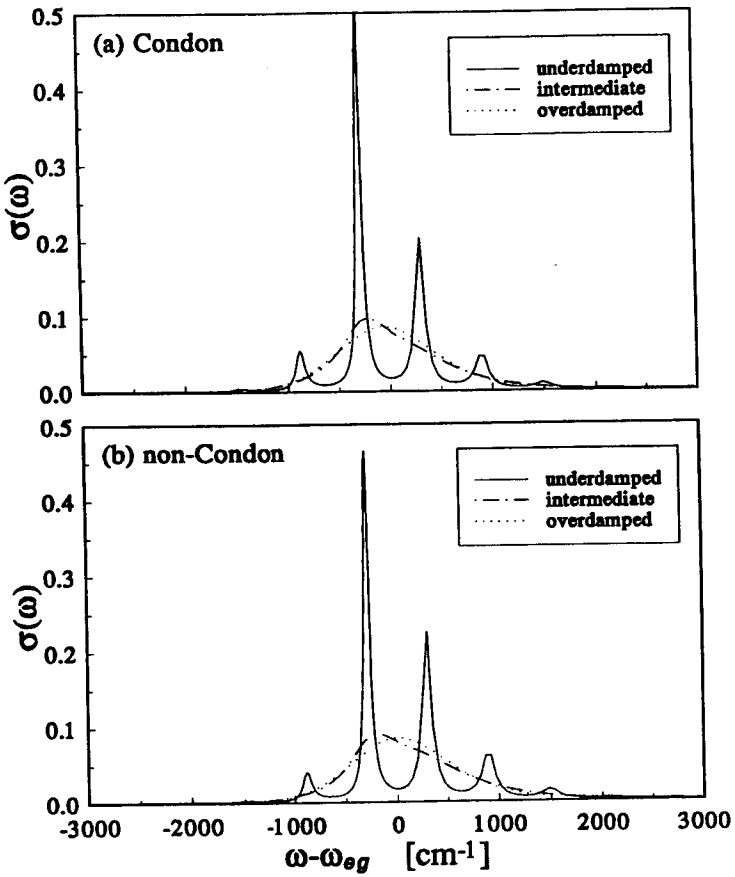

Fig. 1. Absorption spectrum with Condon dipole interaction ($c = 0$) for: 1) the underdamped case, $\gamma = 40$ [cm^{-1}]; 2) the intermediate case $\gamma = 400$ [cm^{-1}]; and 3) the overdamped case $\gamma = 2000$ [cm^{-1}] at different temperatures $T = 100$ [K]. In a) indicate results with Condon approximation ($c = 0$), whereas b) without Condon approximation ($c = 0.1$).

These effects become larger in nonlinear experiments such as pump-probe experiments, since they are higher orders in the dipole interaction.

Figure 2 shows the impulsive pump-probe spectrum for the underdamped case $\gamma = 40$ [cm^{-1}]. Here, we define $\Delta\omega = \omega_2 - \Omega_2 - \omega_{eg}$. Figure 2a is for the Condon approximation whereas 2b is for the non-Condon interaction. In each case, we display separately the contributions of the hole, the particle, and their sum. In Figures 2a and 2b, the particle spectra are rapidly changing in both the Condon and the non-Condon cases; however the hole for the

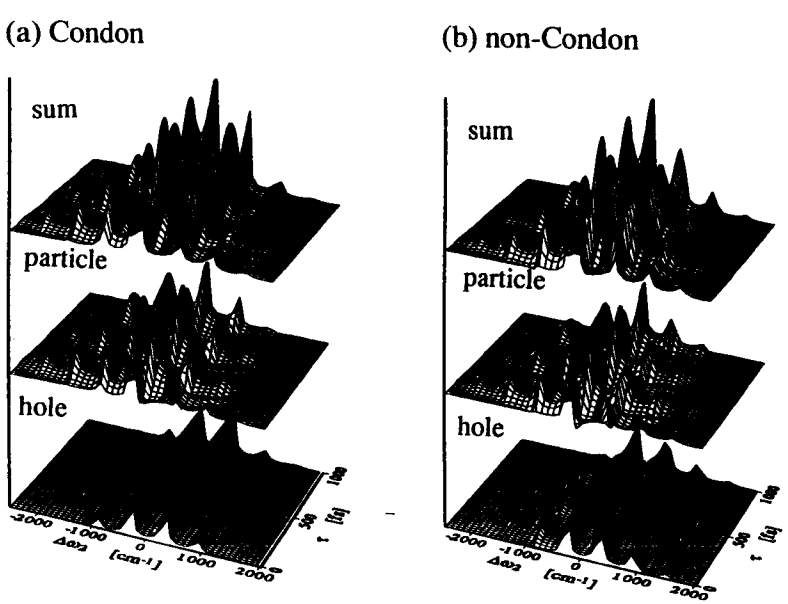

Fig. 2. The impulsive pump-probe spectrum for the underdamped case $\gamma = 40$ [cm^{-1}] at the low temperature $T = 100$ [K]. Here, we define $\Delta\omega = \omega_2 - \Omega_2 - \omega_{eg}$. Figure 2a is for the Condon approximation whereas 2b is for the non-Condon interaction. In each of these, we display separately the contributions of the hole, the particle, and their sum.

Condon case (the bottom of 2a) does not change at all with time. This can be understood by plotting the time evolution of the wavepacket. Figure 3 shows the wavepacket corresponding to Figure 2 (the unit of r is $\sqrt{\hbar/M\omega_0}$). We plotted three wavepackets (the hole, the particle and their sum) as a function of the coordinate and the time. In this underdamped mode, the particle moves from the ground state position $q = 0$ to the equilibrium state $q = d = -1$ (the bottom of the excited state potential) with a coherent oscillation, both for the Condon and the non-Condon cases. However, the hole, which in the Condon case does not change its position and shape, slightly oscillates in the non-Condon case. This is due to the impulsive pump [23]. Under the Condon approximation, the impulsive pump pulse creates a particle in the excited state without changing the Gaussian shape of the wavepacket in the ground-state. Then, the shape of the hole wavepacket is also Gaussian and cannot move in the harmonic potential. However, in the non-Condon case, the coordinate dependent dipole operator affects the shape of the ground equilibrium state.

Figures 4 and 5 show the spectra for the intermediate damping case $\gamma = 400$ [cm^{-1}]. As seen from the middle of Figures of 5a and 5b, the motion

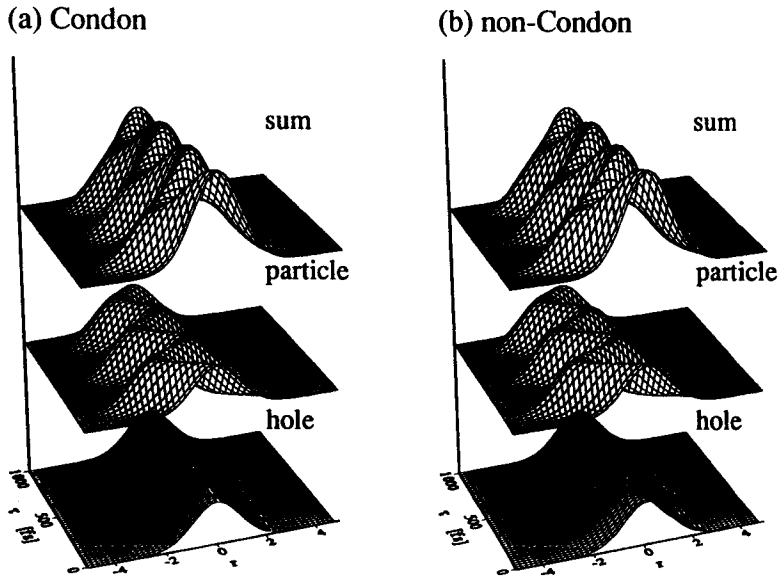

Fig. 3. The time-evolutions of the wavepacket for the underdamped case corresponds to Figure 2 (the unit of r is $\sqrt{\hbar/M\omega_0}$). We plotted three wavepacket (the hole, the particle and the total) as the function of the coordinate and the time.

of the particle is critically damped and the particle quickly moves from the equilibrium position of the ground state ($r = 0$) to the bottom of the excited potential ($r = -1$). These motions are clearly reflected to the spectra Figure 4.

Figures 6 and 7 are for the overdamped damping case $\gamma = 2000$ [cm^{-1}]. In this case, the particle motion is strongly suppressed by the heat bath and particle quickly reaches its equilibrium distribution. Under strong damping, even though with non-Condon interaction, the hole cannot move and shows similar behavior to the Condon case.

Acknowledgements

The support of the National Science Foundation is gratefully acknowledged.

Appendix: Optical Polarization and Wavepackets with Non-Condon Dipole Moment

In order to express the wavepacket element and the optical polarization in compact way, it is convenient to introduce a sign parameter, ε_1, ε_2, and ε_3,

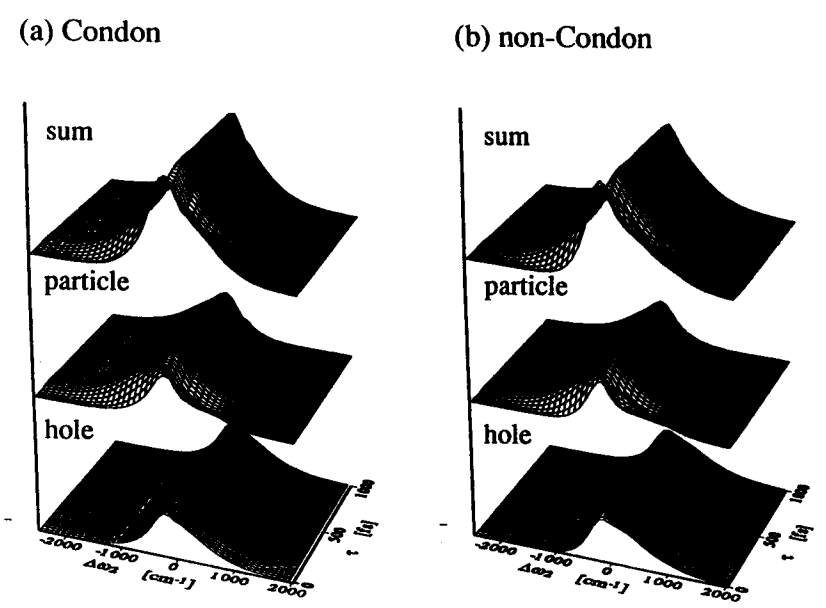

Fig. 4. The impulsive pump-probe spectrum for the intermediate damped case $\gamma = 400$ [cm^{-1}]. The other parameters are the same as the case of Figure 2.

TABLE I

Auxiliary parameters for Equations (A2)–(A15).

Liouville space path α	ε_1	ε_2	ε_3
1	+	+	+
2	−	+	+
3	−	−	+
4	+	−	+

Each Liouville space path is characterized by 3 parameters, as given in Table I. Using these, the first and the third order polarization with the non-Condon

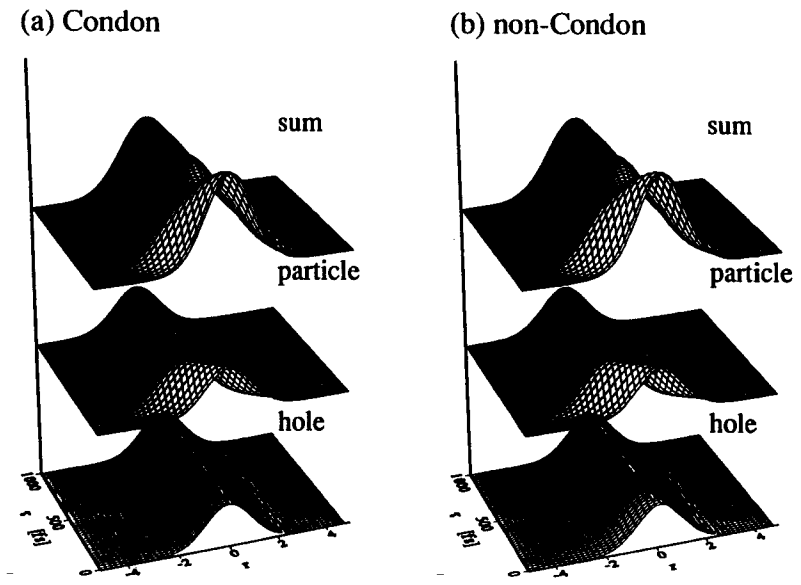

Fig. 5. The time-evolutions of the wavepacket for the intermediate damped case corresponds to Figure 4.

interaction are expressed as [19]

$$P^{(1)}(t) = -i\int_0^\infty dt_1 E(t-t_1)\{\mu(\partial/\partial c_1)\mu(\partial/\partial c_2) R_+^{(1)}(t_1,c_1,c_2)\}|_{c_1=c_2=0} + c.c., \tag{A1}$$

$$P^{(3)}(t) = i\int_0^\infty dt_3 \int_0^\infty dt_2 \int_0^\infty dt_1 E(t-t_3) E(t-t_2-t_3)E(t-t_1-t_2-t_3) \times \sum_{\varepsilon_1\varepsilon_2=\pm} \{\mu(\partial/\partial c_4)\mu(\partial/\partial c_3)\mu(\partial/\partial c_2)\mu(\partial/\partial c_1) R^{(3)}_{\varepsilon_1\varepsilon_2+}(t_3,t_2,t_1,\{c_j\})\}|_{\{c\}=0} + c.c. \tag{A2}$$

Here, the generating function of the non-Condon response functions are defined by

$$R^{(1)}_{\varepsilon_1}(t_1,c_1,c_2) = \exp[Q_{\varepsilon_1}(t_1) + X_{\varepsilon_1}(t_1,c_1,c_2)], \tag{A3}$$

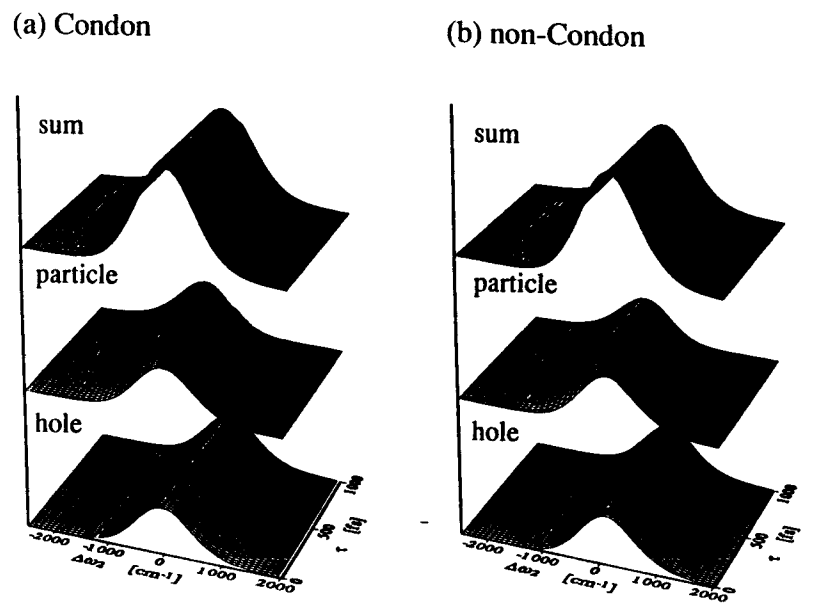

Fig. 6. The impulsive pump-probe spectrum for the overdamped case $\gamma = 2000$ [cm^{-1}]. The other parameters are the same as the case of Figure 2.

$$R^{(3)}_{\varepsilon_1\varepsilon_2\varepsilon_3}(t_3,t_2,t_1;\{c_j\}) = \exp[Q_{\varepsilon_1\varepsilon_2\varepsilon_3}(t_3,t_2,t_1) + X_{\varepsilon_1\varepsilon_2\varepsilon_3}(t_3,t_2,t_1;\{c_j\})], \tag{A4}$$

where

$$Q_{\varepsilon_1}(t_1) = -i\varepsilon_1\omega_{eg}t_1 - g_{-\varepsilon_1}(t_1), \tag{A5}$$

$$\begin{aligned} &Q_{\varepsilon_1\varepsilon_2\varepsilon_3}(t_3,t_2,t_1) \\ &= -i\omega_{eg}(\varepsilon_1 t_1 + \varepsilon_3 t_3) - g_{-\varepsilon_1}(t_1) - g_{\varepsilon_2\varepsilon_3}(t_3) \\ &\quad -\varepsilon_1\varepsilon_3[g_{\varepsilon_1\varepsilon_2}(t_2) - g_{\varepsilon_1\varepsilon_2}(t_2+t_3) \\ &\quad -g_{-\varepsilon_1}(t_1+t_2) + g_{-\varepsilon_1}(t_1+t_2+t_3)], \end{aligned} \tag{A6}$$

$$\begin{aligned} X_{\varepsilon_1}(t_1,c_1,c_2) &= -i\xi^{-1}\dot{g}_{-\varepsilon_1}(t_1)(c_1+c_2) \\ &\quad +\xi^{-2}\left[\ddot{g}_{-\varepsilon_1}(t_1)c_1c_2 + \frac{1}{2}(c_1^2+c_2^2)\ddot{g}(0)\right], \end{aligned} \tag{A7}$$

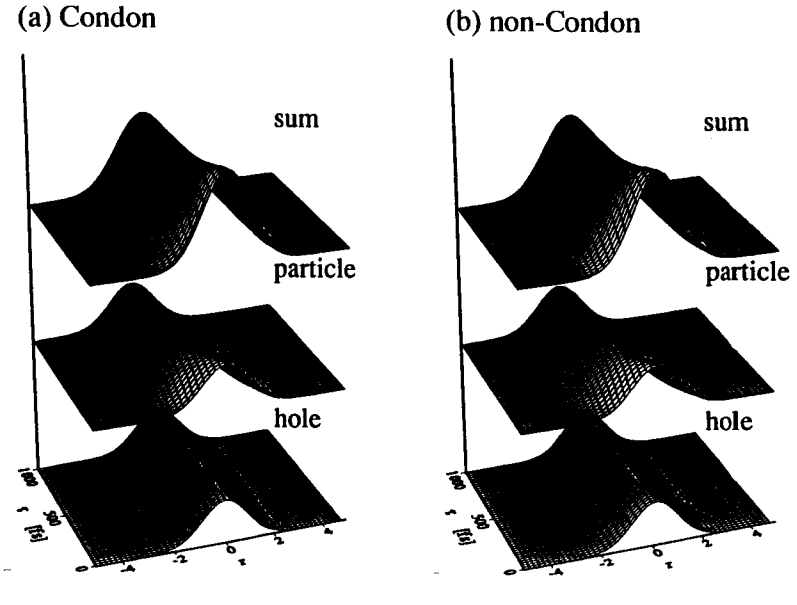

Fig. 7. The time-evolutions of the wavepacket corresponds to Figure 6.

$$\begin{aligned} X_{\varepsilon_1\varepsilon_2\varepsilon_3}(t_3,t_2,t_1,\{c_j\}) &= c_1\langle\bar{q}_1(\{t\})\rangle_{\varepsilon_1\varepsilon_2\varepsilon_3} + c_2\langle\bar{q}_2(\{t\})\rangle_{\varepsilon_1\varepsilon_2\varepsilon_3} \\ &\quad +c_3\langle\bar{q}_3(\{t\})\rangle_{\varepsilon_1\varepsilon_2\varepsilon_3} + c_4\langle\bar{q}_4(\{t\})\rangle_{\varepsilon_1\varepsilon_2\varepsilon_3} \\ &\quad +\xi^{-2}\left[c_1c_2\ddot{g}_{-\varepsilon_1}(t_1) + c_1c_3\ddot{g}_{-\varepsilon_1}(t_1+t_2)\right. \\ &\quad +c_2c_3\ddot{g}_{\varepsilon_1\varepsilon_2}(t_2) + c_1c_4\ddot{g}_{-\varepsilon_1}(t_1+t_2+t_3) \\ &\quad +c_2c_4\ddot{g}_{\varepsilon_1\varepsilon_2}(t_2+t_3) + c_3c_4\ddot{g}_{\varepsilon_2\varepsilon_3}(t_3) \\ &\quad \left.+\frac{1}{2}(c_1^2+c_2^2+c_3^2+c_4^2)\ddot{g}(0)\right], \end{aligned} \tag{A8}$$

with

$$\begin{cases} \langle\bar{q}_1(\{t\})\rangle_{\varepsilon_1\varepsilon_2\varepsilon_3} = -i\xi^{-1}[\varepsilon_1\dot{g}_{-\varepsilon_1}(t_1) - \varepsilon_3\dot{g}_{-\varepsilon_1}(t_1+t_2) \\ \qquad +\varepsilon_3\dot{g}_{-\varepsilon_1}(t_1+t_2+t_3)], \\ \langle\bar{q}_2(\{t\})\rangle_{\varepsilon_1\varepsilon_2\varepsilon_3} = -i\xi^{-1}[\varepsilon_1\dot{g}_{-\varepsilon_1}(t_1) + \varepsilon_3\dot{g}_{\varepsilon_1\varepsilon_2}(t_2+t_3) \\ \qquad -\varepsilon_3\dot{g}_{\varepsilon_1\varepsilon_2}(t_2)], \\ \langle\bar{q}_3(\{t\})\rangle_{\varepsilon_1\varepsilon_2\varepsilon_3} = -i\xi^{-1}[\varepsilon_1\dot{g}_{-\varepsilon_1}(t_1+t_2) - \varepsilon_1\dot{g}_{\varepsilon_1\varepsilon_2}(t_2) \\ \qquad +\varepsilon_3\dot{g}_{\varepsilon_2\varepsilon_3}(t_3)], \\ \langle\bar{q}_4(\{t\})\rangle_{\varepsilon_1\varepsilon_2\varepsilon_3} = -i\xi^{-1}[\varepsilon_1\dot{g}_{-\varepsilon_1}(t_1+t_2+t_3) - \varepsilon_1\dot{g}_{\varepsilon_1\varepsilon_2}(t_2+t_3) \\ \qquad +\varepsilon_3\dot{g}_{\varepsilon_2\varepsilon_3}(t_3)]. \end{cases} \tag{A9}$$

Note that Equations (A5) and (A6) are just a compact expression of Equations (2.22) and (2.28), and are very convenient for numerical evaluations. The first and the third order wavepackets are given by

$$W^{(1)}(p,q,t) = \int_0^\infty dt_1 E(t-t_1)\mu(\partial/\partial c_1)\left(4\pi^2\langle p^2\rangle_g\langle q^2\rangle_g\right)^{-1/2} \times \exp\left[-\frac{1}{2\langle q^2\rangle_g}(q-\bar{q}_+(t_1,c_1))^2 - \frac{1}{2\langle p^2\rangle_g}(p-\bar{p}_+(t_1,c_1))^2\right] R_+^{(1)}(t_1,c_1,c_2)|_{c_1=c_2=0} + c.c., \tag{A10}$$

and

$$\begin{aligned} W^{(3)}(p,q,t) = \int_0^\infty dt_1 \int_0^\infty dt_2 \int_0^\infty dt_3 E(t-t_3)E(t-t_2-t_3) \\ E(t-t_1-t_2-t_3)\mu(\partial/\partial c_1)\mu(\partial/\partial c_2)\mu(\partial/\partial c_3) \\ \times(4\pi^2\langle p^2\rangle_g\langle q^2\rangle_g)^{-1/2}\sum_{\varepsilon_1,\varepsilon_2=\pm} \\ \times\exp\left[-\frac{1}{2\langle q^2\rangle_g}(q-\bar{q}_{\varepsilon_1\varepsilon_2+}(\{t\},\{c\}))^2\right. \\ \left. -\frac{1}{2\langle p^2\rangle_g}(p-\bar{p}_{\varepsilon_1\varepsilon_2+}(\{t\},\{c\}))^2\right] \\ \times R^{(3)}_{\varepsilon_1\varepsilon_2+}(t_3,t_2,t_1;\{c\})|_{\{c\}=0} + c.c. \end{aligned} \tag{A11}$$

where the constants are given in Equation (2.19) and

$$\bar{q}_{\varepsilon_1}(t_1,c_1) = -i\xi^{-1}\dot{g}_{-\varepsilon_1}(t_1) + c_1\xi^{-2}\ddot{g}_{-\varepsilon_1}(t_1), \tag{A12}$$

$$\bar{p}_{\varepsilon_1}(t_1,c_1) \equiv -iM\xi^{-1}\ddot{g}_{-\varepsilon_1}(t_1) + c_1M\xi^{-2}\dddot{g}_{-\varepsilon_1}(t_1), \tag{A13}$$

and

$$\begin{aligned} \bar{q}_{\varepsilon_1\varepsilon_2\varepsilon_3}(\{t\},\{c\}) = -i\xi^{-1}[\varepsilon_1\dot{g}_{-\varepsilon_1}(t_1+t_2+t_3) - \varepsilon_1\dot{g}_{\varepsilon_2\varepsilon_1}(t_2+t_3) \\ +\varepsilon_3\dot{g}_{\varepsilon_2\varepsilon_3}(t_3)] + \xi^{-2}[c_1\ddot{g}_{-\varepsilon_1}(t_1+t_2+t_3) \\ +c_2\ddot{g}_{\varepsilon_2\varepsilon_1}(t_2+t_3) + c_3\ddot{g}_{\varepsilon_2\varepsilon_3}(t_3)], \end{aligned} \tag{A14}$$

$$\begin{aligned} \bar{p}_{\varepsilon_1\varepsilon_2\varepsilon_3}(\{t\},\{c\}) = -iM\xi^{-1}[\varepsilon_1\ddot{g}_{-\varepsilon_1}(t_1+t_2+t_3) - \varepsilon_1\ddot{g}_{\varepsilon_2\varepsilon_1}(t_2+t_3) \\ +\varepsilon_3\ddot{g}_{\varepsilon_2\varepsilon_3}(t_3)] + M\xi^{-2}[c_1\dddot{g}_{-\varepsilon_1}(t_1+t_2+t_3) \\ +c_2\dddot{g}_{\varepsilon_2\varepsilon_1}(t_2+t_3) + c_3\dddot{g}_{\varepsilon_2\varepsilon_3}(t_3)]. \end{aligned} \tag{A15}$$

The second order wavepackets can be obtained from the third order one by simply setting $t_3 = 0$.

References

1. Maroncelli, M., MacInnis, J., and Fleming, G. R., *Science* **234**, 1674 (1989).
2. Barbara, P. F. and Jarzeba, W., *Adv. in Photochem.* **15**, 1 (1990).
3. See "Electron Transfer" Special Issue of *Chem. Rev.* **92** (1992) and references therein.
4. Anfinrud, P. A., Han, C., Lian, T., and Hochstrasser, R. M., *J. Phys. Chem.* **95**, 574 (1991); Owrutsky, J. C., Kin, Y. R., Li, M., Sarisky. M. J., and Hochstrasser, R. M., *Chem. Phys. Lett.* **184**, 368 (1991); Rips, I., Klafter, J., and Jortner, J., *J. Phys. Chem.* **94**, 8557 (1990).
5. Xie, X. and Simon, J. D., *Rev. Sci. Instrumen.* **60**, 2614 (1989).
6. Fourkas, J. T. and Fayer, M. D., *Acc. Chem. Res.* **25**, 227 (1992).
7. Scherer, N. F., Carlson, R. J., Matio, A., Du, M., Ruggiero, A. J., Romero-Rochin, V., Cina, J. A., Fleming, G. R., and Rice, S. A., *J. Chem. Phys.* **95**, 1487 (1991).
8. Nelson, K. A. and Ippen, E. P., *Adv. Chem. Phys.* **75**, 1 (1989).
9. Marcus, R. A., *J. Chem. Phys.* **24**, 966 (1956); **24**, 979 (1956); *Ann. Phys. Chem.* **15**, 155 (1964).
10. Zusman, L. D., *Chem. Phys.* **49**, 295 (1980).
11. Mukamel, S., *Adv. Chem. Phys.* **70**, 165 (1988); Mukamel, S., *Ann. Rev. Phys. Chem.* **41**, 647 (1990).
12. Garg, A., Onuchic, J. N., and Ambegaokar, V., *J. Chem. Phys.* **83**, 4491 (1985).
13. Gruebele, M. and Zewail, A. H., *Phys. Today* **43**, 24 (1990).
14. Yan, Y. J. and Mukamel, S., *J. Chem. Phys.* **94**, 997 (1991); *ibid*, *Phys. Rev.* **A41**, 6485 (1990).
15. Webster, F., Rossky, P. J., and Friesner, R. A., *Comp. Phys.Comm.* **63**, 494 (1991).
16. Tully, J., *J. Chem. Phys.* **93**, 1061 (1990).
17. Sparpaglione, M. and Mukamel, S., *J. Chem. Phys.* **88**, 3263 (1988); *J. Chem. Phys.* **88**, 4300 (1988); Mukamel, S. and Yan, A. J., *Acc. Chem. Res.* **22**, 301 (1989).
18. Feynman, R. P. and Vernon, F. L., *Ann. Phys.* **24**, 118 (1963).
19. Tanimura, Y. and Mukamel, S., *Phys. Rev. E* **47**, 118 (1993); *ibid., J. Opt. Soc. Am. B* (in press).
20. Gehlen, J. N. and Chandler, D., to be published in *J. Chem. Phys.*
21. Grabert, H., Schramm, P., and Ingold, G.-L., *Phys. Rep.* **168**, 115 (1988).
22. Yan, Y. J. and Mukamel, S., *J. Chem. Phys.* **88**, 5735 (1988); **89**, 5160 (1988).
23. Bosma, W. B., Yan, Y. J., and Mukamel, S., *Phys. Rev.* **A42**, 6920 (1990).